

Statistical Mechanics of Tethered Surfaces

Yacov Kantor, Mehran Karċar,^(a) and David R. Nelson

Department of Physics, Harvard University, Cambridge, Massachusetts 02138

(Received 11 June 1986)

We study the statistical mechanics of two-dimensional surfaces of fixed connectivity embedded in d dimensions, as exemplified by hard spheres tethered together by strings into a triangular net. Without self-avoidance, entropy generates elastic interactions at large distances, and the radius of gyration R_G increases as $(\ln L)^{1/2}$, where L is the linear size of the uncrumpled surface. With self-avoidance R_G grows as L^ν , with $\nu = 4/(d+2)$ as obtained from a Flory theory and in good agreement with our Monte Carlo results for $d = 3$.

PACS numbers: 05.40.+j, 64.60.Fr, 82.65.Dp, 87.20.Cn

There is presently considerable understanding of properties of random walks and polymers, obtained through many experimental and theoretical methods.¹ It is therefore natural to generalize the problem from one-dimensional polymers to two-dimensional (2D) surfaces, and there are indeed many recent studies of random surfaces.²⁻⁶ However, in contrast to polymers, there is not a single universality class encompassing all types of surfaces.⁵ Most studies have focused on random surfaces related to high-temperature plaquette expansions of lattice gauge theories.^{2,3} These surfaces are highly ramified, and closely resemble branched polymers.^{2,3,6} But for describing configurations of surfaces commonly encountered in nature such as sheets of covalently bonded atoms, or of polymerized lipid surfaces, a more natural starting point is to consider possible deformations of a *fixed* network of plaquettes,⁴ or of particles placed at the sites of such a network. These latter surfaces are characterized by a fixed internal metric⁵ (e.g., a triangular network), and to distinguish them from other types of surfaces they will be referred to as “tethered,” or “fixed-connectivity,” surfaces. If there are *mobile* disclinations (i.e., points of fivefold and sevenfold coordination in a triangular net, or threefold and fivefold coordination in a square net), then the internal structure of the surface will be “liquid”⁷ and it may resemble more the former random plaquette surfaces.

In this Letter we report some results for surfaces of fixed connectivity. A simple example of such surfaces is a collection of hard spheres tethered by strings of finite extension into a 2D triangular net, embedded in d -dimensional space. In the absence of self-avoiding (SA) restrictions, we find that at large distances the surface behaves elastically, as a result of entropic effects. The analogous result for polymers follows from simple random-walk ideas.¹ For tethered surfaces, we demonstrate this important result via a simple real-space rescaling procedure, and by direct numerical Monte Carlo (MC) simulation. Whereas in the absence of self-avoidance the radius of gyration R_G grows with the linear (uncrumpled) size of the surface L as $R_G^2 \sim \ln L$, for a SA network it increases as $R_G \sim L^\nu$.⁸ A Flory theory¹ gives the estimate ν_F

$= 4/(d+2)$, in good agreement with our numerical simulations of the network embedded in three dimensions (3D). We briefly discuss the static and dynamic properties of these surfaces, and their applicability to physical systems.

Consider a system of particles connected to form a triangular 2D lattice, and embedded in d -dimensional space (the precise 2D lattice is not important, as long as the connections between its sites are fixed). Each particle is labeled by a 2D *internal* coordinate $\mathbf{x} = (x_1, x_2)$ with discrete x_1 and x_2 denoting its place on the network. Its actual location in the embedding space is described by the d -dimensional *external* coordinate $\mathbf{r}(x_1, x_2)$. The Hamiltonian with pairwise nearest-neighbor (nn) interactions is

$$\frac{H}{k_B T} = \sum_{\langle \mathbf{x}, \mathbf{x}' \rangle} V(|\mathbf{r}(\mathbf{x}) - \mathbf{r}(\mathbf{x}')|). \quad (1)$$

Since the SA restrictions between distant parts of the surface are ignored at this stage, Eq. (1) describes a *phantom* network. The statistical mechanics associated with Eq. (1) can be solved exactly for a Gaussian potential $V(r) = \frac{1}{2} K_0 r^2$. The mean value of $|\mathbf{r}(\mathbf{x}) - \mathbf{r}(\mathbf{x}')|^2$, for example, grows as $(d/\pi\sqrt{3}K_0) \ln |\mathbf{x} - \mathbf{x}'|$. Gross⁴ has studied a related model with an elastic energy associated with changes in the areas of elementary triangles. Since R_G^2 in the latter model also grows logarithmically the two models appear to be in the same universality class.

The large-length-scale behavior for other potentials $V(r)$ is less obvious. For (linear) polymers the Markovian nature of the chain enables calculation of the long-wavelength properties.¹ Unfortunately, surfaces cannot be solved in a similar manner, and we must resort to more approximate techniques. One possible rescaling of the network is via the Migdal-Kadanoff bond-moving approximation for integrating out the intermediate particles.⁹ According to this procedure, after rescaling of the *internal* coordinates by a factor b , the *external* potential V renormalizes to $V' = D(bD(bV))$, where $D(V)$ is the dual potential obtained by a Fourier transformation as

$$e^{-D(V(k))} \equiv \int d^d r e^{i\mathbf{k} \cdot \mathbf{r} - V(r)}.$$

Any Gaussian potential is invariant under this transformation, indicating a fixed line. We found numerically that a variety of potentials (including the "rigid rod" potential which forces the neighboring points to remain at a fixed distance, and the hard-sphere-and-string potential which will be discussed later) converge to the Gaussian fixed line under renormalization. The number of iterations of the transformation necessary to approach the Gaussian fixed potential defines a persistence length for the surface, while the renormalized spring constant K_R provides a measure of the large-distance entropy-generated elasticity.

Going beyond the approximate rescaling of the potential, the asymptotic Gaussian behavior was confirmed numerically for a system of hard spheres of unit diameter connected by strings of maximal extent $\sqrt{3}$ [i.e., $V(r)=0$ for $1 < r < \sqrt{3}$, and ∞ otherwise], embedded in 3D. This surface model closely resembles the standard models used to simulate linear polymers.¹⁰ Since our potentials do not introduce an energy scale into the problem, the results are independent of temperature, and the free energy is solely due to entropy effects. Such potentials may be expected to generate small persistence lengths, and thus reduce the crossover effects. The configuration space is sampled by use of the MC (or "Brownian dynamics") method¹¹: During a "basic time step" we attempt to update the position of each atom by adding a vector of length s with randomly chosen direction to its current position. The move is accepted only if the new position of the atom is allowed by the potentials. We use $s=0.2$, for which about half of the attempted moves are accepted. We perform the MC simulations for $L \times L$ parallelograms (in lattice units) with free edges, cut out of a triangular lattice with L ranging from 2 to 16 for phantom surfaces, and from 2 to 11 for SA surfaces (see later). Because the MC procedure generates a highly correlated sequence of configurations, the actual sampling of configurations is made only every $\tau_0 = L^2/s^2$ time steps, and the total length of each simulation is $100\tau_0$. The time τ_0 is proportional to the Rouse relaxation time (see Sect. VI in Ref. 1), during which the free surface "forgets" its initial configuration. Thus, for phantom surfaces we sampled completely independent configurations. The average R_G^2

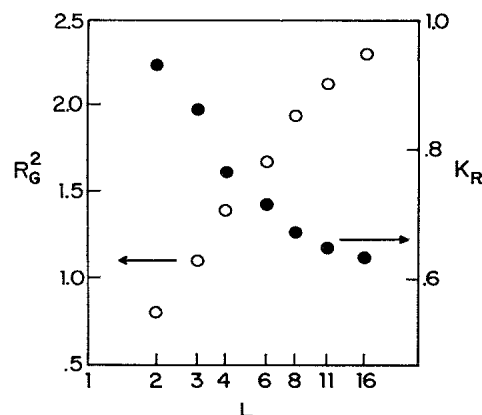


FIG. 1. Semilogarithmic plot of R_G^2 of the free surface (open circles) and of K_R (solid circles) vs L .

of such a surface is depicted in Fig. 1 as a function of its linear size L . The initial slope of the graph is somewhat large, because the hard-core repulsion between the nn's still has a noticeable effect on the overall behavior. Eventually, the curve approaches a simple logarithmic behavior as in the Gaussian model. Figure 1 also depicts the ratio between the measured R_G^2 and that of a Gaussian surface of the same size with $K_0=1$. This ratio approaches a constant, confirming our expectation, with effective force constant $K_R \approx 0.63$. The approximate rescaling procedure outlined in the previous paragraph gave $K_R \approx 0.7$, and a persistence length of about 8 for this potential, both in agreement with the MC results in Fig. 1. Higher-order interactions, such as those embodied in bending energies,¹² complicate both the rescaling calculation and the numerical simulations. On the basis of universality, however, we expect these factors to only modify the persistence length and the force constant, but not to alter the essential appearance of entropy-generated harmonic forces at sufficiently large distances in phantom fixed-connectivity surfaces.

Our next step is to consider more tangible surfaces, with self-avoidance. We first attempt a continuum description of the problem, by generalizing the Edwards model¹³ for polymers. The partition function Z is obtained by summing over all configurations of the surface $\mathbf{r}(\mathbf{x})$ (the 2D internal coordinate \mathbf{x} is now continuous), as

$$Z = \int \mathcal{D} \mathbf{r} \exp \left[-\frac{1}{2} K \int d^2 x (\nabla \mathbf{r})^2 - \nu \int d^2 x d^2 x' \delta^d(\mathbf{r}(\mathbf{x}) - \mathbf{r}(\mathbf{x}')) \right], \quad (2)$$

where $(\nabla \mathbf{r})^2 \equiv (\partial \mathbf{r} / \partial x_1)^2 + (\partial \mathbf{r} / \partial x_2)^2$ represents the continuum version of the Gaussian potential. The elastic coefficient K results from the previously described coarse graining, while the interaction ν measures the "excluded volume" as in the case of polymers.¹ We can carry out a perturbation expansion in ν ¹⁴ about the phantom surface. To the lowest order, the mean value of the squared distance between two points \mathbf{x} and \mathbf{x}' separated by L along the internal coordinates is given by

$$\langle [\mathbf{r}(\mathbf{x}) - \mathbf{r}(\mathbf{x}')]^2 \rangle = \frac{d \ln L}{\pi K} \left[1 + \frac{\pi^2 \nu}{4} \left(\frac{K}{2} \right)^{d/2} \frac{L^4}{(\ln L')^{1+d/2}} \right]. \quad (3)$$

Up to an unimportant coefficient the cutoff length L' is equal to L . The distance increases with ν as expected, but the perturbation term diverges for large $L' \sim L$. By contrast, for polymers a similar expansion is well behaved above $d=4$,^{1,14} allowing a systematic expansion in $\epsilon=4-d$. Equation (3) suggests that self-avoidance can only be neglected for elastic surfaces when $d=\infty$, in agreement with the observation of Gross⁴ that the Hausdorff dimension of the noninteracting surface is infinite.

Divergent perturbation theory implies a nontrivial scaling that can be studied by a Flory-type approximation.¹ Consider a surface of internal size L , occupying a region R_G in d -dimensional space. The entropic energy according to Eq. (2) scales (up to logarithmic corrections) as $\frac{1}{2}KR_G^2$, while the self-repulsion energy scales as $\nu L^4/R_G^d$. Balancing the two energies we find $R_G \sim (\nu/K)^{1/(d+2)}L^{\nu_F}$, with $\nu_F=4/(d+2)$. (For a related calculation see Ref. 5.) In any case, we expect that the exponent ν is bounded from below by $2/d$ (maximally compact surface), and from above by 1 (maximally stretched surface).

To test these predictions, the MC simulations were repeated with SA restrictions (centers of two spheres cannot come closer than their diameter). The maximal string extension of $\sqrt{3}$ ensures complete impen-

etrability of the surface. A typical configuration generated by the simulation is plotted in Fig. 2. To study the scaling properties of these surfaces, the mean squared radius of gyration (Fig. 3, inset) and the Fourier transform of the two-point correlation function $S(k)$ were examined. The structure factor

$$S(\mathbf{k}, L) = (1/L^2) \sum_{\mathbf{x}, \mathbf{x}'} \langle e^{i\mathbf{k} \cdot [\mathbf{r}(\mathbf{x}) - \mathbf{r}(\mathbf{x}')] } \rangle$$

satisfies the scaling form $S(\mathbf{k}, L) = S(kR_G) = S(kL^\nu)$.¹¹ Indeed, as indicated in Fig. 3, the measured $S(k, L)$ for different values of L all collapse into a single function, when plotted against the scaling variable $q = kL^\nu$ with $\nu = 0.83 \pm 0.03$. For intermediate q the scaling function $S(q)$ behaves as $q^{-2/\nu}$, and from the slope in Fig. 3 we estimate $\nu = 0.77 \pm 0.03$. Note that the data for $L=4$ in Fig. 3 suggest that the persistence length in the SA surface is actually smaller than in the phantom case (Fig. 1). To check the validity and the accuracy of the procedure, we repeated the MC calculation for a single chain of atoms (regular polymer). The results of that simulation are also depicted in the inset of Fig. 3. For the polymer we obtain $\nu = 0.64$, which overestimates the known value of ν , but is reasonable in view of the short chains considered. For SA surfaces our overall estimate is a value of $\nu = 0.80 \pm 0.05$, where the error bars indicate our subjective assessment of the possible systematic errors. This result is in good agreement with the value

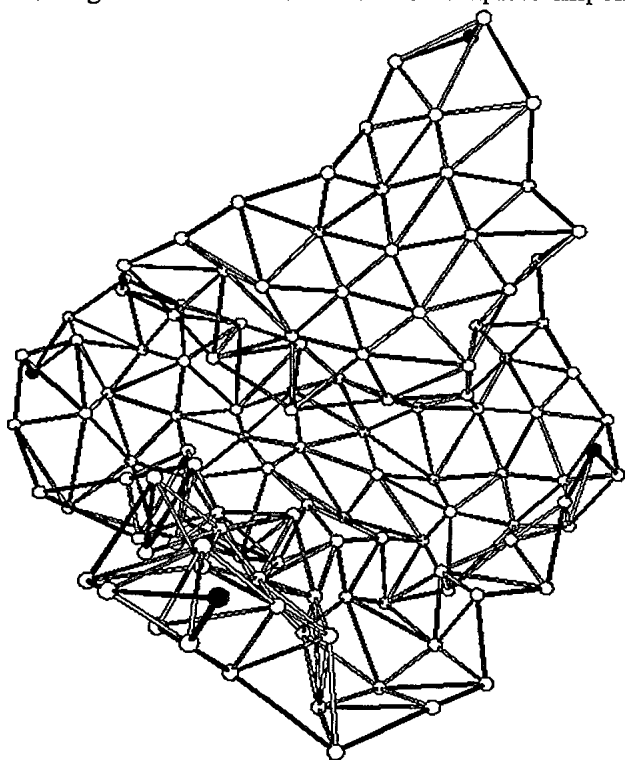


FIG. 2. Shape of the SA surface for $L=11$. For clarity, the sizes of the atoms were taken to be $\frac{1}{5}$ of the actual range of the hard-core potential. Bonds indicate the nn atoms between which the string potential acts. Bonds located at the boundary of the parallelogram and the corner atoms are shown in black.

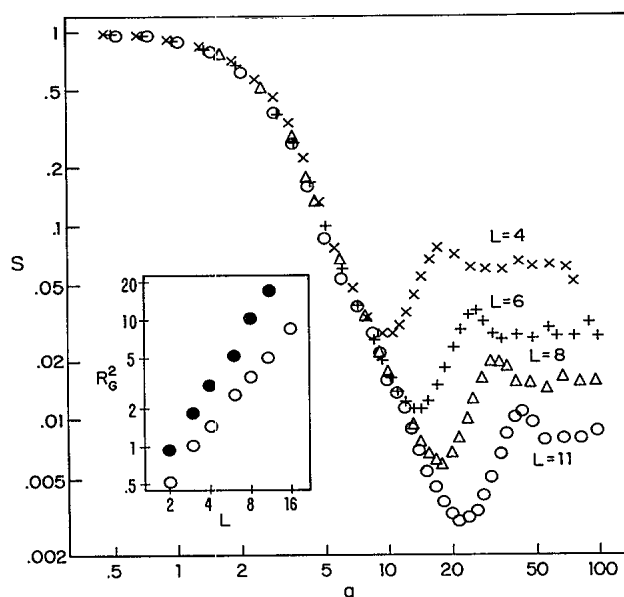


FIG. 3. Logarithmic plot of the structure factor S as a function of $q \equiv kL^\nu$, with $\nu = 0.83$. (Some overlapping data points have been omitted for clarity.) Inset: logarithmic plot of R_G^2 of the SA surface (solid circles) vs L . Symbol sizes are equal to the standard deviation of the R_G^2 . Analogous results for a linear chain are also shown (open circles).

of $\nu_F = \frac{4}{3}$, thus confirming the accuracy of the Flory approximation and the validity of Eq. (2).

As pointed out earlier, for phantom surfaces the Rouse relaxation time $\tau_R(L)$ increases as L^2 . The SA restrictions considerably increase τ , and the independence of the configurations generated by MC simulations had to be checked directly by calculation of various autocorrelation functions (cf. Ref. 11). As in polymers, the relaxation time is bounded by the "reptation" time $\tau_{\text{rep}}(L)$, for the surface to escape from a confining cage, that grows as L^4 (this is just an upper bound, and "reptation" is probably *not* a relaxation mechanism for surfaces). One expects that the relaxation time is now (cf. Ref. 1) $\tau(L) \sim R_g^2 \sim L^{\nu z}$, and for intermediate times $t \ll \tau(L)$, a typical particle displacement $\langle [\mathbf{r}(\mathbf{x}, t) - \mathbf{r}(\mathbf{x}, 0)]^2 \rangle$ grows algebraically as $t^{2/z}$. The exponent z depends on the dynamics imposed on the system. In the Brownian dynamics used for MC simulations $z = 2 + 2/\nu$, while in a fluid, the hydrodynamical interactions result in $z = 3$.

Laboratory examples of surfaces discussed in this Letter are provided by 2D polymer networks (2D gels¹). Some lipid molecules polymerize into sheets with multiple crosslinks upon exposure to ultraviolet radiation.¹⁵ A bilayer of this kind with the polar head groups facing out would presumably enter an aqueous solvent and provide another example of the surfaces studied here. Light-scattering experiments from dilute solutions would yield direct information on the exponent ν and the dynamical fluctuations of individual surfaces. In dense solutions surfaces do not interpenetrate and (unlike regular polymers) are far from ideal. The situation is somewhat like a dense polymer melt in two dimensions. Our results may also be relevant to 2D network glasses, like As_2S_3 or B_2O_3 .¹⁶ Just above the glass transition, the liquid presumably consists of many crumpled sheets of covalently bonded molecules. Understanding the statistical mechanics of an isolated sheet is a first step towards dealing with this problem. The large increase in volume (about 30%) of molten B_2O_3 relative to its crystalline form may be related to the swelling of an isolated surface discussed here.¹⁷ We also carried out a "table-top experiment" by actually irreversibly crumpling sheets of foil. By this rather ill-defined procedure we again measured an exponent $\nu \approx 0.8$.

Our previous results naturally imply that a straight line of length l drawn on the fully extended surface will occupy a volume of size $l^{4/5}$. A SA walk on the extended surface occupies a region of size $l^{3/4}$. Upon crumpling, the walk will extend over a size $(l^{3/4})^\nu \sim l^{3/(d+2)}$, which, remarkably, coincides with the Flory prediction for polymers in d dimensions ($d \leq 4$)! Also, for a strip of width w and length l , we may ob-

serve a crossover from SA polymers to tethered surfaces, for which Flory theory predicts (for $d \leq 4$ and $w < l$) a scaling form $R_G \sim (wl^3)^{1/(d+2)}$. More details of our results will appear in future communications.

We would like to acknowledge conversations with G. Blackburn, M. E. Cates, P. Ginzparg, K. Kremer, D. Turnbull, and T. A. Witten. We are indebted to D. Vanderbilt for help on the graphics and other features of the Apollo computer. This research was supported by the National Science Foundation through the Harvard Material Science Laboratory and through Grant No. DMR 85-14638. One of us (M.K.) acknowledges support from the Harvard Society of Fellows.

(a)Present address: Physics Department, Massachusetts Institute of Technology, Cambridge, MA 02139.

¹P. G. de Gennes, *Scaling Concepts in Polymer Physics* (Cornell Univ. Press, Ithaca, NY, 1979).

²J.-M. Drouffe, G. Parisi, and N. Sourlas, Nucl. Phys. B161, 397 (1979).

³For a review see J. Fröhlich, in *Applications of Field Theory to Statistical Mechanics*, edited by L. Garido, Lecture Notes in Physics Vol. 216 (Spring-Verlag, Berlin, 1985).

⁴A. Billoire, D. J. Gross, and E. Marinari, Phys. Lett. 139B, 75 (1984); D. J. Gross, Phys. Lett. 139B, 187 (1984).

⁵M. E. Cates, Phys. Lett. 161B, 363 (1985), and Phys. Rev. Lett. 53, 926 (1984).

⁶U. Glaus, Phys. Rev. Lett. 56, 1996 (1986), and references therein.

⁷D. R. Nelson, Phys. Rev. B 26, 269 (1982), and references therein.

⁸Our definition of ν is twice that used in Refs. 3 and 6.

⁹L. P. Kadanoff, Ann. Phys. (N.Y.) 100, 359 (1976). A similar procedure appears in A. N. Berker and D. R. Nelson, Phys. Rev. B 19, 2488 (1979).

¹⁰A. Baumgärtner, in *Applications of the Monte Carlo Method in Statistical Physics*, edited by K. Binder (Springer-Verlag, Berlin, 1984), p. 145, and references therein.

¹¹D. Ceperley, M. H. Kalos, and J. L. Lebowitz, Phys. Rev. Lett. 41, 313 (1978).

¹²W. Helfrich, Z. Naturforsch. 28c, 693 (1973); P. G. de Gennes and C. Taupin, J. Phys. Chem. 86, 2294 (1982); L. Peliti and S. Leibler, Phys. Rev. Lett. 54, 1690 (1985), and references therein.

¹³S. F. Edwards, Proc. Phys. Soc. London 85, 613 (1965).

¹⁴M. Fixman, J. Chem. Phys. 23, 1656 (1955); J. des Cloizeaux, J. Phys. (Paris) 42, 635 (1981).

¹⁵See, for example, papers cited in Thin Solid Films 68 (1980), and 99 (1983).

¹⁶R. Zallen, *The Physics of Amorphous Solids* (Wiley, New York, 1983), Chap. 3.

¹⁷D. Turnbull, private communication. See also M. J. Aziz, E. Nygren, J. F. Hays, and D. Turnbull, J. Appl. Phys. 57, 2233 (1985).